DOI：10.19789/j.1004-9398.2026.05.005　　**Open Access**
文献引用：王之祎，吴若曦，张明浩，等．利用盐溶液对太赫兹脉冲进行高性能检测[J]．首都师范大学学报（自然科学版），2026，47（5）：30-36.
Wang Zhiyi，Wu Ruoxi，Zhang Minghao，et al. High-performance detection of terahertz pulses utilizing aqueous salt solutions[J]. Journal of Capital Normal University（Natural Science Edition），2026，47（5）：30-36.

利用盐溶液对太赫兹脉冲进行高性能检测*

王之祎[1]，吴若曦[1]，张明浩[1]，张存林[1]，张亮亮[1,2**]

（1. 首都师范大学物理系太赫兹光电子学教育部重点实验室，北京　100048；
2. 深圳市龙华先进技术检测研究院，广东 深圳　518000）

摘要：基于液态水的太赫兹探测方法具有优越的性能，可以改善固体和空气基探测方案中带宽有限、激光能量要求高的问题。相较于纯水，盐溶液也能显著提高检测性能。本文报道了基于盐溶液的太赫兹探测方法，系统研究了不同离子电荷对探测灵敏度的影响。结果表明，盐溶液性能均显著优于纯水，具有较大的三阶非线性系数和较低的电离势。该方案提升了太赫兹探测液体的性能，为利用太赫兹技术探究不同液体的物理化学性质提供了支撑。

关键词：太赫兹波；盐溶液；相干探测
中图分类号：O441.4　　**文献标志码**：A

High-performance detection of terahertz pulses utilizing aqueous salt solutions*

Wang Zhiyi[1]，Wu Ruoxi[1]，Zhang Minghao[1]，Zhang Cunlin[1]，Zhang Liangliang[1,2**]

（1. Key Laboratory of Terahertz Optoelectronics，Department of Physics，Capital Normal University，Beijing　100048；2. Detection Institute for Advanced Technology Longhua-Shenzhen，Shenzhen Guangdong　518000）

Abstract：Terahertz detection methods based on liquid water have superior performance and can alleviate the problems of limited bandwidth and high laser energy requirements in solid- and air-based detection schemes. Compared with pure water，aqueous salt solutions can also significantly improve the detection performance. This paper reports aqueous salt solutions based terahertz detection method and systematically investigates the effect of varying ionic charges on detection sensitivity. The results show that aqueous salt solutions consistently outperform pure water remarkably，with larger third-order nonlinear coefficients and lower ionization potentials. This scheme improves the performance of terahertz detection liquids，providing support for exploring the physical and chemical properties of different liquids using terahertz technology.

Keywords：terahertz wave；aqueous salt solutions；coherent detection
CLC：O441.4　　**DC**：A

收稿日期：2025-10-10
*北京市教委科技发展计划项目（23JD0035）；北京市青年学者计划项目；深圳市龙华区科创委项目（20250113G43468522）
**通信作者：liangliang_zhang@cnu.edu.cn

0 Introduction

Terahertz (THz) wave pertains to the frequency ranging from 0.1 to 10.0 THz (with a corresponding wavelength of 3 000 to 30 μm) within the electromagnetic wave spectrum. The utilization of this frequency band can broaden human comprehension of certain fundamental scientific issues in astronomy, chemistry, physics, informatics, and life sciences. THz technology finds extensive applications in radar, remote sensing, homeland security and counter-terrorism[1-3], high-security data communication and transmission[4], atmospheric and environmental monitoring[5-6], real-time biological information extraction[7], medical diagnosis[8-13], and other domains. Therefore, research on THz detection technology possesses substantial economic and security implications for the nation.

Common THz detection methods include solid-based[14-15], gas-based[16], and liquid-based detection[17]. Solid-based detection relies on photoconductive antenna and electro-optic sampling technology[18]. Nevertheless, the non-instantaneous response of the dielectric carrier, along with its capacity for phonon absorption, makes it challenging to extend the detection bandwidth of the material to cover the entire terahertz band. Gas-based detection remains unaffected by these factors[19]. The coherent detection of sufficiently wide terahertz waves can be accomplished through air-biased coherent detection and optically-biased coherent detection. However, to attain sufficiently high detection sensitivity, it is typically necessary to employ a probe laser beam with energy of several hundred microjoules. The broadband THz coherent detection technology based on water has been demonstrated to exhibit outstanding performance, which can alleviate the issues of limited bandwidth and high requirements for laser energy in solid- and air-based detection schemes. The third-order nonlinear coefficient of aqueous salt solutions is higher than that of pure water[20-21], which can further enhance detection sensitivity and the signal-to-noise ratio. The physicochemical properties of different salt solutions vary significantly[22-25]. Researchers have investigated these properties in the terahertz band using terahertz spectroscopy, ultrafast infrared spectroscopy, and terahertz Kerr effect[26-28]. In 2022, Zhang et al[29] demonstrated that the detection method based on liquid water can be extended to salt solutions. Therefore, the water-based detection method has been adapted for use with aqueous salt solutions[20-21], which can generate more detection signals and significantly enhance sensitivity.

In this paper, we employed a liquid detection method to detect THz signals by substituting water with aqueous salt solutions that share the same cation but different anions. For a given cation in a brine solution, the larger the ionic radius, the weaker the ion-water binding energy and the greater the sensitivity. This approach significantly improves detection efficiency.

1 Theoretical

1.1 Scaling law of coherent detection signal strength

The coherent detection mechanism based on liquid generates terahertz induced second harmonic (TISH) through the four-wave mixing process. According to reference [19], the liquid-based detection mechanism is based on the TISH generation via the four-wave mixing process, where two fundamental laser beams and a THz beam are superimposed to produce a second harmonic beam. Among them, the relationship between the TISH field E_{TISH}, the THz field E_{THz}, and the fundamental frequency detection laser field E_{ω} is expressed as $E_{\mathrm{TISH}} \propto \chi^{(3)} E_{\omega}^{2} E_{\mathrm{THz}}$, and $\chi^{(3)}$ is the third-order nonlinear susceptibility. To achieve coherent detection, a controlled second harmonic (CSH) field E_{CSH} must spatially and temporally overlap with the TISH field. At the time point t_{THz}, the detection signal can be represented as an interference of two second harmonic (SH) fields, and the resulting signal is described by the following equation

$$S_{2\omega}\left(t_{\mathrm{THz}}\right) \propto \int_{-\infty}^{+\infty} \left| E_{\mathrm{TISH}} + E_{\mathrm{CSH}} \right|^{2} \mathrm{d}t \propto$$

$$\int_{-\infty}^{+\infty} \left| \chi^{(3)} E_{\omega}^{2}\left(t - t_{\mathrm{THz}}\right) E_{\mathrm{THz}}\left(t\right) \right|^{2} \mathrm{d}t +$$

$$\int_{-\infty}^{+\infty} E_{\mathrm{CSH}}\left(t-t_{\mathrm{THz}}\right) E_{\mathrm{CSH}}^{*}\left(t-t_{\mathrm{THz}}\right) \mathrm{d}t + 2\mathrm{Re}\left\{\int_{-\infty}^{+\infty} \chi^{(3)} E_{\omega}^{2}\left(t-t_{\mathrm{THz}}\right) E_{\mathrm{CSH}}^{*}\left(t-t_{\mathrm{THz}}\right) E_{\mathrm{THz}}(t) \mathrm{d}t\right\}. \quad (1)$$

The first term pertains to the process of incoherent detection, while the second term addresses direct current (DC) noise, which can be eleminated through the use of a chopper and a phase-locked amplifier. The third term relates to the coherent detection process. Due to the fact that the first term $\left|\chi^{(3)} E_{\omega}^{2} E_{\mathrm{THz}}\right| \ll |\chi^{(3)} E_{\omega}^{2} E_{\mathrm{CSH}}^{*} E_{\mathrm{THz}}|$ is much smaller than the third term, making the signal predominantly consist of the coherent component. Considering that the maximum SH conversion efficiency of the BBO crystal is about 5%, the energy of the CSH beam can reach about 0.5 μJ with a probe laser energy of 10 μJ. We have demonstrated that coherent detection can be achieved with just 1.55×10^{-2} μJ of CSH energy, even for a THz field with an intensity as high as 100 MV/cm[19]. This feature makes it ideal for correlation detection.

Equation (1) shows that the coherent detection signal intensity depends linearly dependent on $\chi^{(3)}$, which is significantly affected by the solution's refractive index η. The refractive index can be defined as $\eta = \eta_0 + \eta_2 I$, where η_0 is the linear refractive index, η_2 is the nonlinear refractive index, and I is the light intensity. The relation between η_2 and $\chi^{(3)}$ is given by reference[30]. The refractive index, and consequently the detection signal strength of these solutions, is directly proportional to both the refractive index and the concentration of solid salts, showing a quadratic relationship. As solution concentration increases, detected signal strength rises correspondingly due to the higher refractive index associated with increased concentrations. The solution's refractive index (η_0) is proportional to that of the solid salt (η_s) and its concentration C[20,31]. With increasing solution concentration, the relationship between $\chi^{(3)}$, η_0 and η_s can be expressed as

$$\chi^{(3)} \propto \eta_0^2 \propto C\eta_s^2. \quad (2)$$

Here, the correlation between the THz detection signal and $\chi^{(3)}$ or η_0 of aqueous salt solutions has been established. This can be extended to other liquids and serves as a simple guideline for assessing the nonlinear susceptibility of various liquids.

1.2 Calibration rule of incoherent detection signal strength

The first term of equation (1) corresponds to the incoherent detection component, which can be measured separately under the condition that $\left|\chi^{(3)} E_{\omega}^{2} E_{\mathrm{THz}}\right| \gg |\chi^{(3)} E_{\omega}^{2} E_{\mathrm{CSH}}^{*} E_{\mathrm{THz}}|$. If the CSH beam is not used in the experiment, the incoherent detection can be easily achieved. In this case, the detected signal contains only a TISH beam,

$$S_{\mathrm{TISH}}\left(t_{\mathrm{THz}}\right) \propto \int_{-\infty}^{+\infty} \left|\chi^{(3)} E_{\omega}^{2}\left(t-t_{\mathrm{THz}}\right) E_{\mathrm{THz}}(t)\right|^{2} \mathrm{d}t. \quad (3)$$

According to equations (2) and (3), one can easily obtain[19]

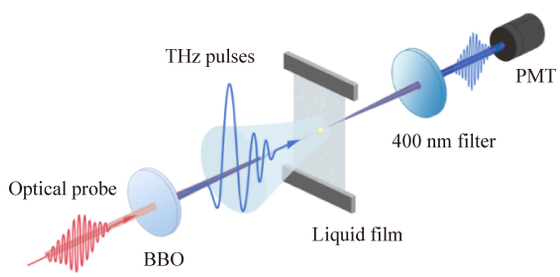
$$S_{\mathrm{TISH}} \propto \left[\chi^{(3)}\right]^{2} \propto \eta_0^4 \propto C^2\eta_s^4. \quad (4)$$

Equation (4) demonstrates that the linear refractive index of solid salt in various solutions exhibits an approximate fourth power relationship with the intensity of the incoherent detection signal.

2 Experimental setup

The schematic diagram of our experimental setup is illustrated in figure 1. In this study, we utilized a 1 550 nm laser beam, and an organic crystal of 4-N, N-dimethylamino-4'-N'-methylstilbazoliumtosylate (DAST) was employed to generate a strong THz pulse with a maximum electric field strength of 5 MV/cm. The THz pulse and the 800 nm femtosecond probe beam are both polarized in the vertical direction and are simultaneously focused onto a free-flowing liquid film. When the energy of the probe beam surpasses 2 μJ, this configuration leads to the formation of a liquid plasma. The 400 nm SH beam emitted from the liquid plasma is subsequently collected through a 400 nm narrow band filter and directed onto a photomultiplier tube (PMT) for observation. When a 100 μm thick type I barium β-borate (BBO) crystal is positioned in the path of an 800 nm probe beam, a CSH can be generated and propagated coaxially with the fundamental beam. When a vertically polarized CSH beam is coherent with a TISH

beam，a linear component that exhibits a positive correlation with the THz field emerges in the collected signal. In the experiment，a micro-peristaltic pump generated pressure to eject liquid from a flat needle at approximately 80 mL/min. This created a stable flowing film with a thickness of about 50 μm and a width of 3 mm. This dimension exceeds the spot size of the THz beam. All measurements were taken at an ambient temperature of（22 ± 1）℃.



Note：BBO denotes β-borate；PMT denotes photomultiplier tube.

Figure 1　experimental device system diagram

3　Experimental results and discussion

We conducted coherent THz detection experiments using eight different aqueous salt solutions. All aqueous salt solutions were prepared at a concentration of 4 mol/L，except for the CsI solution，which had a saturation concentration of 2 mol/L. Other experimental conditions remained consistent across various aqueous salt solutions and pure water. The time-domain waveforms of THz fields for NaCl，NaBr，NaI，and water detected in sodium aqueous salt solutions are presented in figure 2（a）. Detection performance was enhanced in brine solutions with all three types of sodium compared to pure water（black curve）. We observe a clear order of detection performance：NaI > NaBr > NaCl > H_2O. Notably，the sensitivity of the NaI solution is about 1.8 times greater than that of pure water. The increase in the detected signal was attributed to the addition of salt ions. The varying sensitivities of sodium brine solutions are due to different anions.

The experimental results for potassium and cesium aqueous salt solutions are shown in figure 2（b，c），respectively. Note that CsBr solution was excluded from this experiment due to its high toxicity. Similarly，the detection performance in potassium and cesium brine solutions is greater than that observed in pure water，which aligns with findings from sodium brine solution. We believe that the enhancement of the detection signal should be attributed to the enhancement of the third-order nonlinear polarizability $\chi^{(3)}$ of the liquid with the addition of ions.

To further investigate the parameters associated with detection performance，we plotted the peak signal intensity as a function of the linear refractive index of solid salts in various solutions，as illustrated in figure 3（a）. Here，we examine the refractive indices of eight solid salts at a frequency of 9 THz[32]，which falls within the frequency range of the THz source utilized in our experiment.

It is evident that in the figure，the refractive index of iodide is generally higher than that of bromide and chloride. Additionally，the inorganic salt containing Cs^+ exhibits a larger refractive index within this group. For instance，CsI exhibits the highest refractive index among iodides，which correlates with its largest

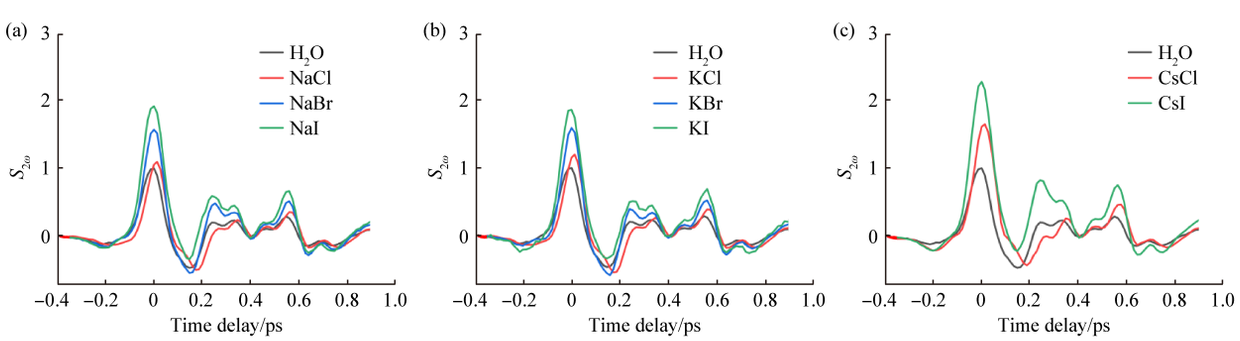


Figure 2　coherent detection of THz pulses in liquid films

（a）aqueous salt solutions of sodium；（b）aqueous salt solutions of potassium；（c）aqueous salt solutions of cesium

detection signal. Additionally, CsCl not only possesses the highest refractive index within chlorides but also surpasses that of bromides. We fitted the experimental results to the specified refractive index. The red dotted line illustrates the fitted data, whereas the black data points represent the detection signal intensities of various types of inorganic salts. The variation in the intensity of the detection signal is proportional to the square of the refractive index of the inorganic salt crystal within the THz frequency range. This aligns with the theory presented in equation(2). Subsequently, the concentration of the aqueous salt solutions was modified, and the experimental results are presented in the figure 3(b-d), shows that the coherent detection signal strength increases with the increase of solution concentration C. This phenomenon can be elucidated by equation(2).

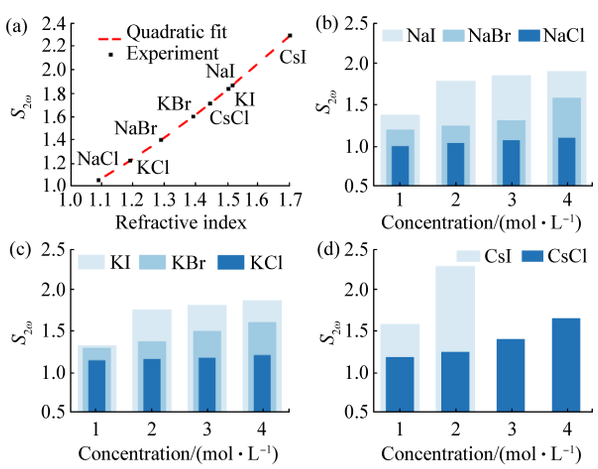


Figure 3 coherent detection intensity of various brine solutions

(a)relationship between peak signal intensity and refractive index;(b)different concentrations of sodium brine;(c)potassium brine;(d)cesium brine

Figure 4(a-c) presents a comparative analysis of incoherent detection across various aqueous salt solutions. The TISH energy signals detected in sodium, potassium, and cesium aqueous salt solutions are provided respectively, along with the TISH energy signals obtained from pure water for reference. It can be observed that when the cation remains constant, an increase in the radius of the anion results in a more pronounced TISH signal and enhances detection performance equation(4) can explain the approximate quartic scale results of the incoherent detection signal strength of different solutions and their respective refractive indices. The experimental findings agree with theoretical predictions.

From the experimental results, we found that the enhancement of the detection signal in salt solution is also related to the radius of anions. The potential energy associated with the interaction between the full charge of the ion and the two partial charges of a water molecule is denoted as $E_{\mathrm{P}} \propto \left(-|z|\mu\right)/r^2$, where z represents the charge number of the ion, μ signifies the electric dipole moment of the water molecule, and r denotes the distance separating the ion from the dipole. The larger the ionic radius, the greater the distance between ions. It is evident that the binding energy of ions is closely associated with their ionic radius. Due to the anion radius relationship as follows: Cl^- (181 pm) < Br^- (196 pm) < I^- (220 pm)[33]. By comparing the THz intensity of aqueous salt solutions, it can be observed that for ions with the same positive charge, a larger anion radius is associated with a weaker ion-water binding energy, thus enhancing performance. The specific correlation needs further study.

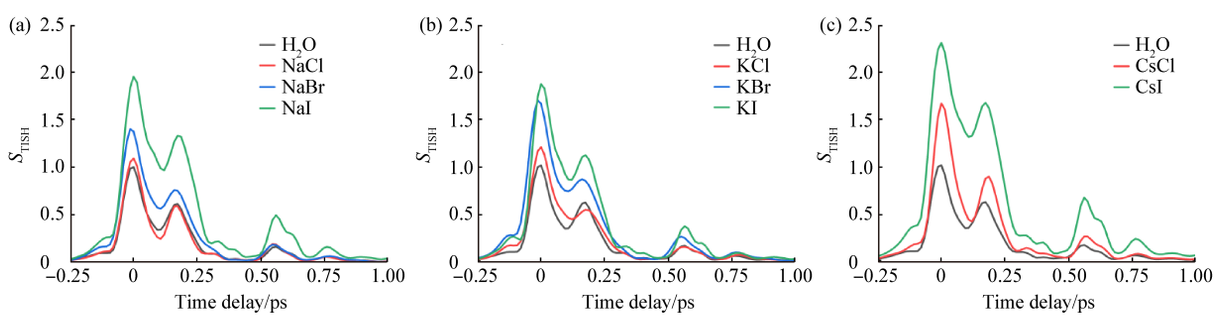


Figure 4 TISH energy signals from different salt solutions

(a)sodium brine;(b)potassium brine;(c)cesium brine

4 Conclusion

In summary, we find that the detection performance of broadband THz pulses can be substantially enhanced by substituting water with aqueous salt solutions. For a given cation in a brine solution, the larger the ion radius, the weaker the ion-water binding energy and the greater the performance. Secondly, a correlation has been established between the THz detection signal and the $\chi^{(3)}$ or η_0 of aqueous salt solutions. This relationship can be generalized to encompass a broader range of liquid types and serves as a practical guideline for assessing the nonlinear sensitivity of various liquids. This study not only presents a methodology to enhance the performance of liquid THz detection but also offers a viable approach for investigating the physicochemical properties of various liquids within the THz frequency range.

©The editorial department of Journal of Capital Normal University (Natural Science Edition) 2025. This is an open access article under the CC BY-NC-ND 4.0 license (https://creativecommons.org/licenses/by-nc-nd/4.0/).

References

[1] Melinger J S, Harsha S S, Laman N, et al. Temperature dependent characterization of terahertz vibrations of explosives and related threat materials[J]. Optics Express, 2010, 18(26): 27238. DOI: 10.1364/oe.18.027238.

[2] Ergün S, Sönmez S. Terahertz technology for military applications[J]. Journal of Military and Information Science, 2015, 3(1): 13. DOI: 10.17858/jmisci.58124.

[3] Palka N, Szala M, Czerwinska E. Characterization of prospective explosive materials using terahertz time-domain spectroscopy[J]. Applied Optics, 2016, 55(17): 4575. DOI: 10.1364/ao.55.004575.

[4] Deng Q Z, Zhang L, Lyu Z D, et al. Private communication with photonic terahertz chaos[J]. Advanced Photonics, 2024, 6(6): 066004. DOI: 10.1117/1.ap.6.6. 066004.

[5] 吴亮, 凌福日, 刘劲松, 等. 太赫兹光谱技术在气体检测中的应用[J]. 激光与光电子学进展, 2009, 46(7): 29. DOI: 10.3788/LOP20094607.0029.
Wu Liang, Ling Furi, Liu Jinsong, et al. Detection of gases with terahertz spectroscopy techniques[J]. Laser & Optoelectronics Progress, 2009, 46(7): 29.

[6] Li S L, Lei L, Gao T C, et al. Research progress of THz technology application in the atmospheric sounding field[J]. Infrared and Laser Engineering, 2016, 45(11): 1125001. DOI: 10.3788/irla201645.1125001.

[7] Peng Y, Shi C J, Zhu Y M, et al. Qualitative and quantitative analysis algorithms based on terahertz spectroscopy for biomedical detection[J]. Chinese Journal of Lasers, 2019, 46(6): 0614002. DOI: 10.3788/cjl201946.0614002.

[8] Woodward R M, Wallace V P, Pye R J, et al. Terahertz pulse imaging of ex vivo basal cell carcinoma[J]. Journal of Investigative Dermatology, 2003, 120(1): 72-78. DOI: 10.1046/j.1523-1747.2003.12013.x.

[9] Fitzgerald A J, Berry E, Zinov'ev N N, et al. Catalogue of human tissue optical properties at terahertz frequencies[J]. Journal of Biological Physics, 2003, 29(2): 123-128. DOI: 10.1023/A:1024428406218.

[10] ScarfÌ M R, RomanÒ M, Di Pietro R, et al. THz exposure of whole blood for the study of biological effects on human lymphocytes[J]. Journal of Biological Physics, 2003, 29(2): 171-176. DOI: 10.1023/A:1024440708943.

[11] Oh S J, Kim S H, Bin Ji Y, et al. Study of freshly excised brain tissues using terahertz imaging[J]. Biomedical Optics Express, 2014, 5(8): 2837. DOI: 10.1364/boe.5.002837.

[12] Joseph C S, Yaroslavsky A N, Neel V A, et al. Continuous wave terahertz transmission imaging of nonmelanoma skin cancers[J]. Lasers in Surgery and Medicine, 2011, 43(6): 457-462. DOI: 10.1002/lsm.21078.

[13] Cheon H, Yang H J, Lee S H, et al. Terahertz molecular resonance of cancer DNA[J]. Scientific Reports, 2016, 6: 37103. DOI: 10.1038/srep37103.

[14] Cai Y, Brener I, Lopata J, et al. Coherent terahertz radiation detection: Direct comparison between free-space electro-optic sampling and antenna detection[J]. Applied Physics Letters, 1998, 73(4): 444-446. DOI: 10.1063/1.121894.

[15] Harter T, Muehlbrandt S, Ummethala S, et al. Silicon-plasmonic integrated circuits for terahertz signal generation and coherent detection[J]. Nature Photonics, 2018, 12: 625-633. DOI: 10.1038/s41566-018-0237-x.

[16] Lu X F, Karpowicz N, Chen Y Q, et al. Systematic study of broadband terahertz gas sensor[J]. Applied Physics Letters, 2008, 93(26): 261106. DOI: 10.1063/1.3056119.

[17] Dai J M, Xie X, Zhang X C. Detection of broadband terahertz waves with a laser-induced plasma in gases[J].

Physical Review Letters, 2006, 97(10): 103903. DOI: 10.1103/physrevlett.97.103903.

[18] 梁达川, 王锴. 太赫兹时域频谱技术研究[J]. 光电技术应用, 2017, 32(4): 1-7. DOI: 10.3969/j.issn.1673-1255.2017.04.001.
Liang Dachuan, Wang Kai. Research on terahertz time-domain spectroscopy technology[J]. Application of Optoelectronic Technology, 2017, 32(4): 1-7.

[19] Tan Y, Zhao H, Wang W M, et al. Water-based coherent detection of broadband terahertz pulses[J]. Physical Review Letters, 2022, 128(9): 093902. DOI: 10.1103/physrevlett.128.093902.

[20] Débarre D, Beaurepaire E. Quantitative characterization of biological liquids for third-harmonic generation microscopy[J]. Biophysical Journal, 2007, 92(2): 603-612. DOI: 10.1529/biophysj.106.094946.

[21] Kucia W E, Sharma G, Joseph C S, et al. Optical Kerr effect of tRNA solution induced by femtosecond laser pulses[J]. Chemical Physics Letters, 2016, 662: 132-136. DOI: 10.1016/j.cplett.2016.09.027.

[22] Kaminsky M. Ion-solvent interaction and the viscosity of strong-electrolyte solutions[J]. Discussions of the Faraday Society, 1957, 24: 171-179.

[23] McAllister R A. The viscosity of liquid mixtures[J]. AIChE Journal, 1960, 6(3): 427-431. DOI: 10.1002/aic.690060316.

[24] Lazzús J A. A group contribution method to predict the melting point of ionic liquids[J]. Fluid Phase Equilibria, 2012, 313: 1-6. DOI: 10.1016/j.fluid.2011.09.018.

[25] Ryckaert J P, Bellemans A. Molecular dynamics of liquid *n*-butane near its boiling point[J]. Chemical Physics Letters, 1975, 30(1): 123-125. DOI: 10.1016/0009-2614(75)85513-8.

[26] Freysz E, Degert J. Terahertz Kerr effect[J]. Nature Photonics, 2010, 4: 131-132. DOI: 10.1038/nphoton.2010.14.

[27] Zhao H, Tan Y, Zhang R, et al. Anion-water hydrogen bond vibration revealed by the terahertz Kerr effect[J]. Optics Letters, 2021, 46(2): 230. DOI: 10.1364/ol.409849.

[28] Tan Y, Zhao H, Zhang R, et al. Ultrafast optical pulse polarization modulation based on the terahertz-induced Kerr effect in low-density polyethylene[J]. Optics Express, 2020, 28(23): 35330. DOI: 10.1364/oe.408555.

[29] Zhang M H, Xiao W, Wang W M, et al. Highly sensitive detection of broadband terahertz waves using aqueous salt solutions[J]. Optics Express, 2022, 30(21): 39142. DOI: 10.1364/oe.472753.

[30] Nie W J. Optical nonlinearity: phenomena, applications, and materials[J]. Advanced Materials, 1993, 5(7/8): 520-545. DOI: 10.1002/adma.19930050704.

[31] Tokarz D, Cisek R, Prent N, et al. Measuring the molecular second hyperpolarizability in absorptive solutions by the third harmonic generation ratio technique[J]. Analytica Chimica Acta, 2012, 755: 86-92. DOI: 10.1016/j.aca.2012.09.049.

[32] Li H H. Refractive index of alkali halides and its wavelength and temperature derivatives[J]. Journal of Physical and Chemical Reference Data, 1976, 5(2): 329-528. DOI: 10.1063/1.555536.

[33] Chen L G, Ren G H, Liu L Y, et al. Terahertz signatures of hydrate formation in alkali halide solutions[J]. The Journal of Physical Chemistry Letters, 2020, 11(17): 7146-7152. DOI: 10.1021/acs.jpclett.0c02046.

(责任编辑:兰丽丽)